Available online at www.sciencedirect.com
SCIENCE DIRECT®
Tunnelling and Underground Space Technology 21 (2006) 690–695
Tunnelling and Underground Space Technology
incorporating Trenchless Technology Research
www.elsevier.com/locate/tust

Technical note

Single fluid jet-grout strength and deformation properties

S. Coulter [a], C.D. Martin [b,*]

[a] Thurber Engineering Ltd., Edmonton, Alta., Canada T6E 6A5
[b] Department of Civil and Environmental Engineering, University of Alberta, Edmonton, Alta., Canada, T6G 2W2

Received 5 July 2005; received in revised form 4 December 2005; accepted 11 December 2005
Available online 24 February 2006

Abstract

The use of sub-horizontal jet-grout columns in the construction of soft ground tunnels is a popular method to provide excavation support. The sequential installation of jet-grout columns in a tunneling environment will result in the jet-grout columns being loaded in a staged manner, resulting in the jet-grout material properties and installation order affecting the magnitude and distribution of surface settlements and face deformations. A laboratory program was carried out to quantify the short-term (<24 h) development of strength and stiffness of a grout with a composition similar to that found in the construction of jet-grout columns. The laboratory tests were conducted at 8 °C to simulate the ground temperatures. Also the laboratory test cylinders were insulated to simulate the boundary condition differences between 600-mm-diameter jet-grout columns in soil and the 76-mm-diameter laboratory samples.

Keywords: Jet-grout columns; Grout strength; Grout stiffness

1. Introduction

The use of jet-grouting in the construction of shallow tunnels is becoming increasingly common, particularly for large tunnels with non-circular profiles. This method uses the installation of a set of sub-horizontal jet-grout columns to form an arch of cemented soil ahead of the tunnel face to provide excavation support (Pelizza and Peila, 1993). The jet-grout arches are installed in stages to provide a series of overlapping partial cone sections (Fig. 1).

In an urban environment one of the design requirements for shallow tunnels is that the construction method must control surface settlement within specified tolerances. However, with jet-grouting there is a delay between the installation of the jet-grout slurry and the hardening of soil–cement mixture. If this hardening is sufficiently delayed the jet-grout column may not have sufficient shear strength to resist the overburden loads resulting in excessive settlement above the tunnel and associated face deformations. Because jet-grout columns are usually installed in groups of four or more (see Fig. 1c), this method would appear to have the potential to induce surface settlements if strict quality control procedures are not adhered too.

An assessment of the development of the strength and stiffness of jet-grout could help to overcome this potential problem. With the knowledge of how the jet-grout hardens the sequencing of the installation could be done such that the excavation loads induced by the installation of a jet-grout column are carried by previous jet-grout column installations that have hardened. Sequencing in this manner where the excavation loads are supported by the jet-grout columns with the greatest degree of hardening would provide greater surface settlement control and excavation support.

A laboratory testing program was carried out to determine the short-term (<24 h) development of the strength and stiffness of a grout mix with a composition similar to that used in the construction of jet-grout columns for tunnel support. In particular, the laboratory tests were conducted at a typical ground temperature (8 °C) rather than

* Corresponding author. Tel.: +1 780 492 2332; fax: +1 780 492 8198.
E-mail address: derek.martin@ualberta.ca (C.D. Martin).

0886-7798/$ - see front matter © 2006 Elsevier Ltd. All rights reserved.
doi:10.1016/j.tust.2005.12.136

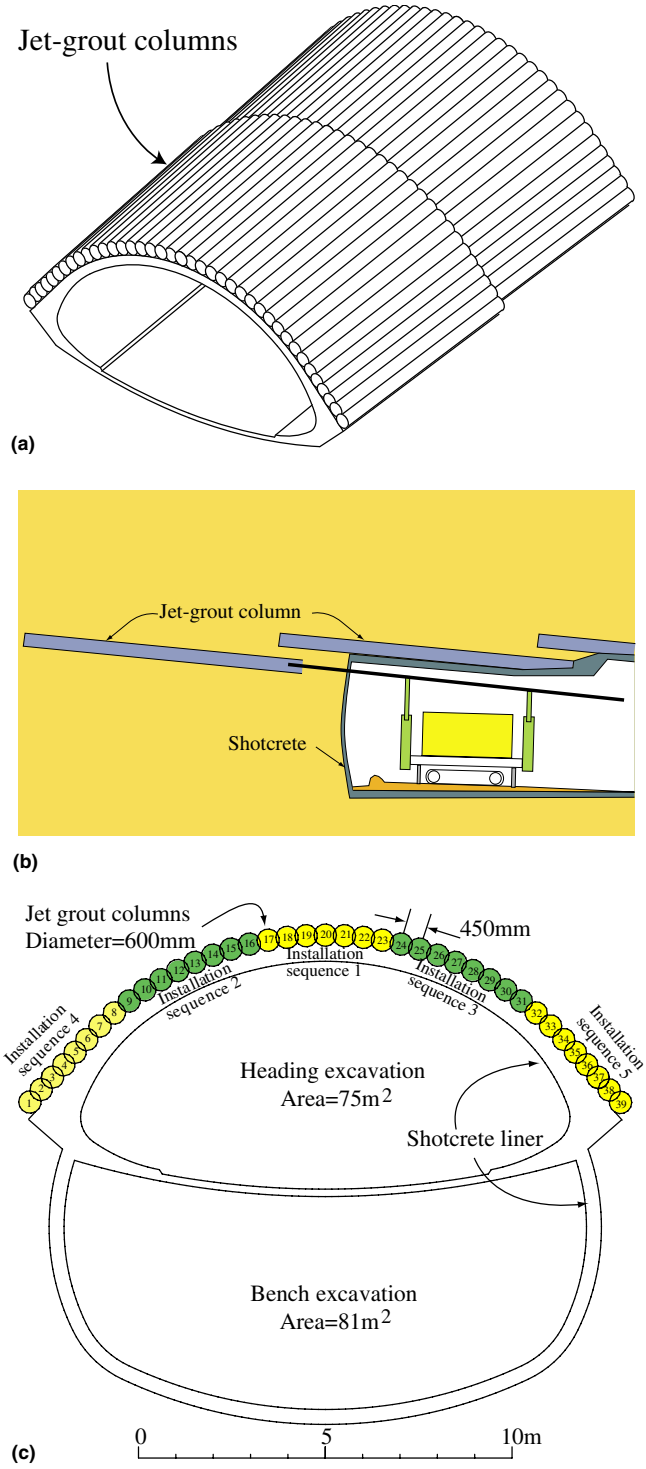

Fig. 1. A typical jet-grout protective umbrella used for a large shallow tunnel. (a) 3D view of jet-grout umbrella; (b) typical longitudinal section showing the jet-grout columns providing the protective umbrella and (c) typical installation sequence for jet-grout column umbrella.

the normal room temperature of 20 °C. Also the laboratory test cylinders were insulated to simulate the boundary condition differences between the 600-mm-diameter jet-grout columns and the 76-mm-diameter laboratory samples. This paper summarizes the time-dependent material properties of jet-grout from these laboratory tests.

2. Jet-grouting background

Jet-grouting was developed in Japan in the 1970s and later introduced in Europe, and by the 1980s it was in use in North America (Brill et al., 2003). In contrast to permeation grouting, which is very sensitive to the type of soils being treated, jet-grouting can be used to treat almost any soil (Bruce et al., 1987). The original system used single fluid system of grout comprised of Portland cement and water. The single fluid system can produce columns up to 500–1000 mm in diameter and is typically used to construct sub-horizontal jet-grout columns in tunneling (Kauschinger et al., 1992).

Jet-grouting is performed in two phases (Mussger et al., 1987). In the first phase, the drill string is advanced by rotary drilling. In the second phase, the jetting is started and the drill string is rotated and withdrawn.

2.1. Composition of jet-grout

The composition of jet-grout is partially dependent on the soil being treated. The analytical calculation of the composition of jet-grout is not possible in practice because of the complex processes of erosion, mixing, replacement, filling of pore space and the jet-grouting parameters (Croce and Flora, 2000). The prediction of the jet-grout composition must then be based upon observations. Croce and Flora (2000) found that the percent soil removal ranged from 30% to 60% in field trials of single fluid jet-grouting in sandy gravel and silty sand (see Table 1).

2.2. Behavior of jet-grout

Fully hardened jet-grout behaves much like Portland cement concrete, i.e., it generally has a non-linear elastic response followed by a brittle failure. Its strength has both a cohesive and a frictional component, e.g., Fang et al. (1994) determined using triaxial tests that the cohesion and friction angle of jet-grout in silty sands was 4.2 MPa and 35°, respectively. While the properties of fully hardened jet-grout can be readily determined, understanding the process of the development of strength in jet-grout requires an understanding of the hydration process of Portland cement.

The hydration of Portland cement is an exothermic reaction, and as such the rate of reaction is partially dependant

Table 1
Typical parameters used during jet-grouting operations

Parameter	Range	Typical
Borehole diameter (mm)	76–115	
Number of jets	2–4	
Nozzle diameter (mm)	1.5–3	2
Grout pump pressure (MPa)	30–60	40
Grout mix (water:cement)	0.8–2.0:1	1:1
Drilling rod rotation rate (RPM)	10–20	15
Withdrawal rate (m/min)	0.25–0.5	0.4
Grout injection rate (m^3/h)	5–8	

upon the reaction temperature. As the reactants are consumed (water and Portland cement) heat is released as the hydrated products are formed. These hydrated products, called the gel, contribute to the strength of hardened Portland cement. Although the amount of heat released depends on the degree of hydration, the composition of the hydration products depends upon the curing temperature (Taylor, 1990). This suggests that the strength of Portland cement is dependent on the time–temperature path of the hydration state.

The hydration of cement pastes exhibits at least two and sometimes three cycles of heat generation (Fig. 2). The first cycle is produced immediately after the mixing of the cement with water due to the hydration of tricalcium aluminate (C_3A). The rate of heat generation reaches a maximum at about 5 minutes and then rapidly falls off due to the water becoming saturated with gypsum. The first cycle is followed by a period of 1–6 h, where the rate of heat generation is very low (Bye, 1983). During this low period, the rheology of the paste remains fairly constant. The second cycle is due to the hydration of tricalcium silicate (C_3S). The peak heat generation in this cycle is observed between 6 and 10 h (Bye, 1983). The decrease in the rate of heat generation after this peak is due to two causes: (1) the decreasing amount of reactants (C_3S), and (2) the inhibiting effect of the calcium silicate hydrates (CSH) gel coating the remaining reactants (the cement particles). The initial set occurs when the CSH gel begins to interlock between cement particles on the rising side of this second cycle (Bye, 1983). Because these temperature effects can impact the hardening and properties of the jet-grout, the laboratory program described in the following section, was specially designed to simulate in situ heat generation.

3. Laboratory testing of jet-grout properties

To characterize the properties of jet-grout, 41 specimens were tested to determine the development of strength and stiffness as a function of time. The testing focused on the period from the initial setting to 24 h of curing. The Young's modulus, uniaxial compressive strength, and Brazilian tensile strength were tested at approximately 6, 7, 8.5, 10.5, 13.75, 18.5 and 24 h, and also at 2, 3 and 28 days.

3.1. Testing procedure

The water to cement ratio of the jet-grout tested was 1:1 by weight. The grout was proportioned to be the same as jet-grouting with 50% soil removal. The aggregate was silty-sand from a glacial outwash deposit in the Edmonton, Canada area and the cement was Canadian Standards Association (CSA) Type 30, a high-early strength Portland cement.

The grout samples were cast in 76 mm inner diameter by 305 mm long acrylic tubes (Fig. 3). The tubes were encased in polystyrene insulation with a 200 mm outer diameter. Plastic spacers, 19 mm thick were inserted into the acrylic tubes 152 mm apart so that a 2:1 height to diameter ratio sample would be obtained. The spacers were used so that samples with smooth square ends would be produced. This eliminated the need to cap or cut the samples. The spacers had two 12 mm holes to enable the placement of the grout. The imperfections on the ends of the samples resulting from these holes were easily removed with a metal scraper.

The polystyrene insulation was provided so that the laboratory tests would have a similar time–temperature

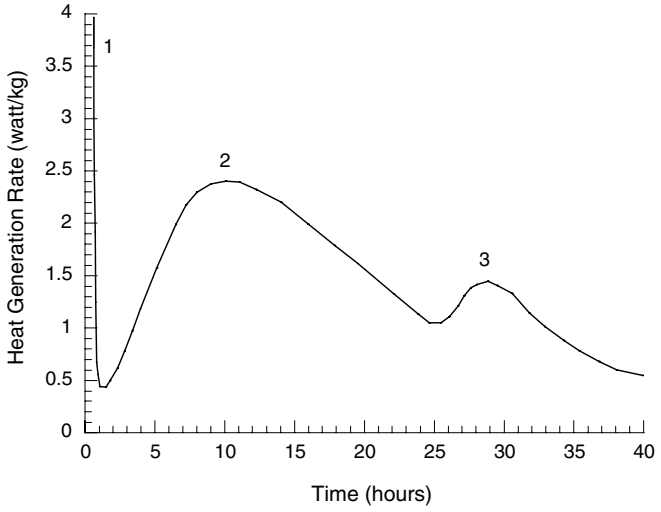

Fig. 2. Heat generation rate for isothermal hydration for normal Portland cement at room temperature, data from Taylor (1990).

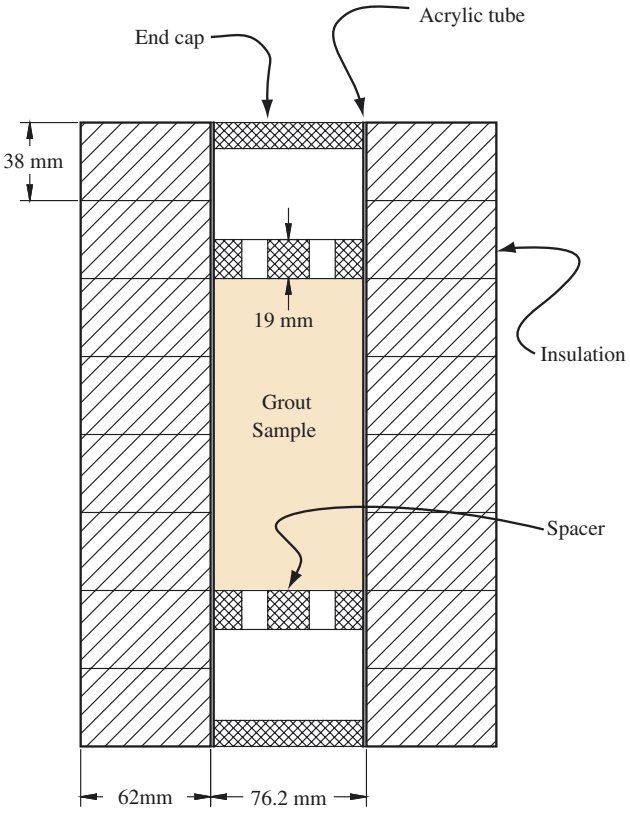

Fig. 3. Configuration of the grout mould used to create the laboratory samples.

history as a jet-grout column installed in the field. This was necessary because of the dependency of the strength of hardened cement on the time–temperature history that it experiences. The curing of the grout was performed in a temperature-controlled room with an ambient temperature of 8 °C, and temperature of the grout recorded with thermistors during hydration. The temperature of 8 °C was chosen as it is similar to ground temperatures encountered in shallow tunneling in many temperate countries.

The required thickness of the insulation was determined using the finite difference method to simulate radial heat flow from a cylindrical source (600-mm-diameter jet-grout column in the field versus 76-mm-diameter grout sample in the laboratory) into an insulator (soil in the field versus polystyrene insulation in the laboratory). Coulter (2004) showed that the 200 mm outer diameter of polystyrene insulation was required for the grout in the laboratory to have a similar average temperature history as the jet-grout column in the field for the initial 24-h period. This amount of insulation provided a laboratory simulated temperature history that had an average temperature over 24 h of 3.5% higher than the field simulation. The thermal properties used in the finite difference model are shown in Table 2. Coulter (2004) conducted a sensitivity analysis of the finite difference matching technique to the thermal properties used in the analysis and concluded that the errors generated were less than 10%.

3.2. Testing results

The testing results showed that the grout had an initial set at approximately 6 h after initial mixing. At this time the grout had sufficient strength so that the 76-mm-diameter samples were capable of being removed from the moulds without significant damage, although they were still soft enough to be indented by careless handling. Hardening of the grout was rapid following this, with the greatest rates of hardening in the first 24 h. Additionally, there appeared to be a transition in the nature of the grout at approximately 11 h. At this time the material behavior changed from plastic to brittle, the rate of increase of the unconfined compressive strength and the Young's modulus reached a peak, and the rate of temperature increase was a maximum.

The unconfined compressive strength (UCS) was observed to initially increase with time with a power-type relationship, i.e, the rate of strength gain was increasing with time. This is observed in Fig. 4a as the straight line portion up to approximately 10.5 h at which time the rate of strength gain is at its greatest. Beyond 10.5 h, the rate of strength gain slows with time. The 28-day strength has a mean of 14.2 MPa with a standard deviation of 0.75 MPa.

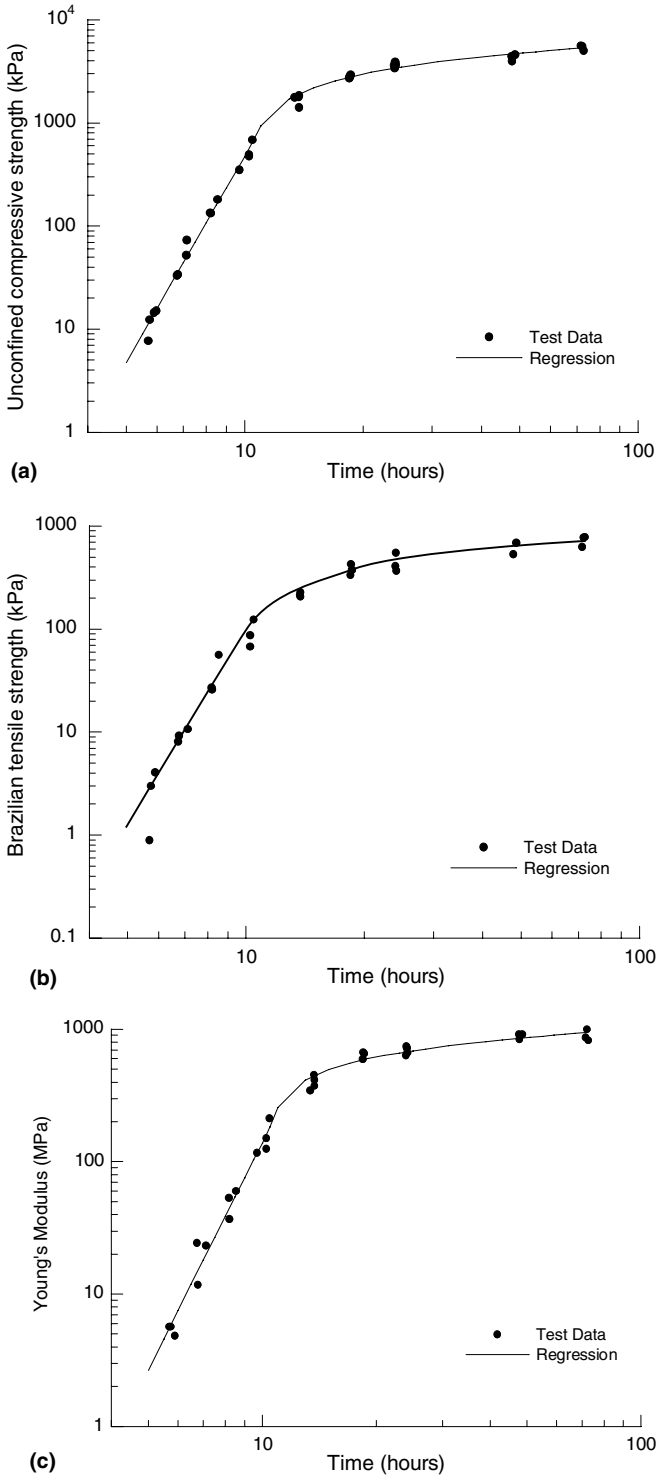

Fig. 4. Development of the unconfined compressive strength, Brazilian tensile strength and the tangent Young's modulus with time. (a) Uniaxial compressive strength; (b) Brazilian tensile strength and (c) Young's modulus.

Table 2
Thermal properties used in the finite difference model

Material	k kJ/(m °C)	C_ρ kJ/(m^3 °C)
Grout	0.00125	2625
Insulation	0.000032	41
Sand	0.0025	2500

Eq. (1) represents the strength for times less than 10.5 h and Eq. (2) represents the strength for times greater than 10.5 h. The units for time (t) are in hours and the units for unconfined compressive strength (UCS) are in kPa.

$$\text{UCS} = 1.088 \times 10^{-4} t^{6.638} \quad < 10.5\text{ h} \tag{1}$$

$$\text{UCS} = 1088 \ln(t - 8.34) - 408.7 \quad > 10.5\text{ h} \tag{2}$$

Vane shear tests were also carried out to determine the shear strength between 3.5 and 5.5 h. These tests gave shear strength ranging from approximately 1 kPa at 3.5 h to approximately 20 kPa at 5.5 h. The strength gain can be approximated by Eq. (3).

$$\text{Vane shear strength} = 1.1 \times 10^{-4} t^{7.1} \tag{3}$$

where the units for time (t) are in hours and the units for the vane shear strength are in kPa.

The tensile strength development with time (Fig. 4b) had a similar shape as the unconfined compressive strength development in Fig. 4a, but with slightly more scatter in the data. The average ratio of tensile strength to compressive strength was 0.133.

The Young's modulus was calculated as the tangent stiffness at 50% peak strength. The development of the Young's modulus with time also has a similar shape as the development of UCS with time (Fig. 4c). Eq. (4) represents the Young's modulus for times less than 10.5 h and Eq. (5) represents the modulus for times greater than 10.5 h. The units for time (t) are in hours and the units for the Young's modulus (E) are in MPa.

$$E = 1.088 \times 10^{-4} t^{5.697} \quad < 10.5\text{ h} \tag{4}$$

$$E = 184.3 \ln(t - 9.51) + 183.7 \quad > 10.5\text{ h} \tag{5}$$

The relationship between uniaxial compressive strength and Young's modulus is shown in Fig. 5. This relationship can also be observed in the stress–strain curves in Fig. 6. The stress–strain behavior of the samples tested at times less than 10.5 h is shown in Fig. 6a. These samples have a ductile post-peak behavior. The transition to a brittle type of failure appears to occur at 10.5 h, when the unconfined compressive strength is approximately 650 kPa. Fig. 6b clearly shows a brittle response and that the strain to failure increases with increasing peak strength, illustrating how the rate of strength gain is greater than the rate of stiffness gain.

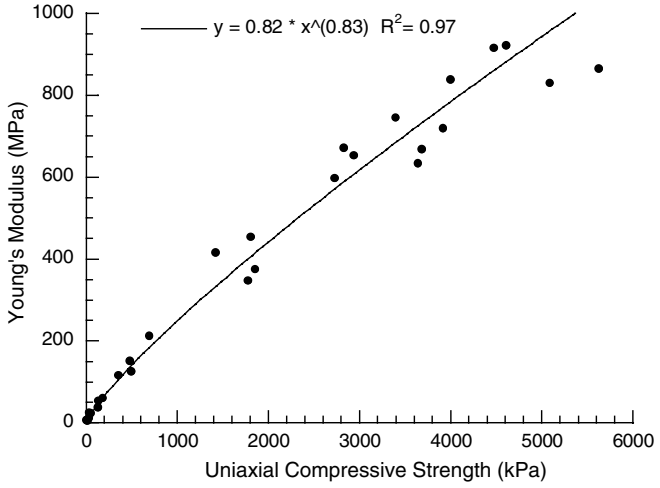

Fig. 5. Relationship between uniaxial compressive strength and Young's modulus.

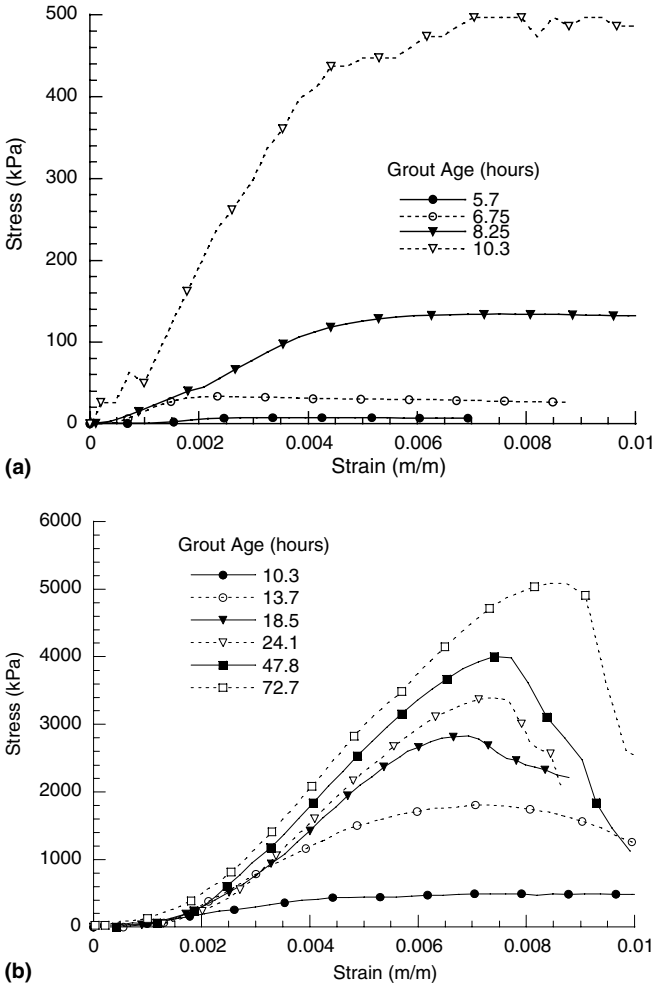

Fig. 6. Stress–strain curves recorded for the unconfined compressive tests for grout at various times. (a) Less than 10.5 h and (b) greater than 10.5 h.

The mean room temperature during the course of the testing was 8.3 °C, with a standard deviation of 0.25 °C. As shown in Fig. 7a, the first cycle of hydration raises the grout temperature by 8.8 °C and occurs in the first hour after mixing. This is followed by approximately 5 h of steady temperature and then a significant temperature gain between 5 and 15 h. The rate of temperature gain reaches a peak value at approximately 11 h (Fig. 7b).

The strong correlation between the change in grout strength and temperature change can be seen by comparing Figs. 4 and 7. The significant strength gain occurs during the second cycle of hydration, i.e., between 5 and 15 h. It is likely that at times less than 6 h the hydration does not contribute to significant strength gain because the cement gel is still discontinuous.

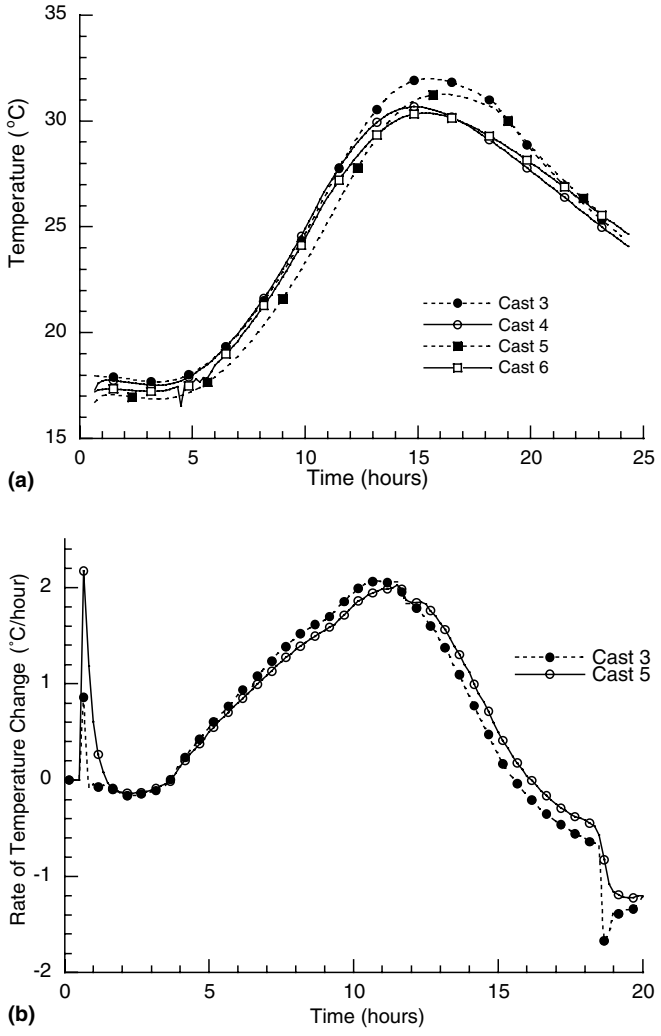

Fig. 7. Grout temperature change recorded at various times. (a) Temperature change with time and (b) rate of temperature change.

4. Discussion

A laboratory testing program was carried out to evaluate the properties of a typical grout mixed used in the installation of horizontal jet-grout columns that form a protective umbrella for tunnel construction and support. The scale difference between the 600-mm-diameter jet-grout columns and the 76-mm-diameter laboratory samples was overcome by placing the laboratory samples in an insulating cylinder in a chamber kept at a constant temperature. A finite difference technique was used to determine the thickness of the insulation such that the heat generation and transfer to the soil was properly simulated in the laboratory conditions. The initial temperature of the laboratory samples and the curing chamber was kept at 8 °C, to simulate the temperature of the ground encountered in shallow tunneling in many temperate countries.

The laboratory results clearly show a 6-h period prior to the onset of hardening. At this stage the grout has essentially no measurable uniaxial compressive strength or stiffness. After this 6-h period there is a very rapid increase in strength and stiffness which continues up to approximately 12 h after initial mixing. After this the hardening process continues, but at a slower rate. The strength and stiffness properties all show a strong correlation with temperature and hence temperature measurements in the field may be a useful indicator for estimating strength and stiffness.

Surface settlements and face deformations can be controlled using horizontal jet-grout columns for excavation support (Mussger et al., 1987; Pelizza and Peila, 1993). However, as indicated by this study the timing and sequencing of the jet-grout installations must be linked to the strength and deformation properties of the grout. Sufficient time must be allowed between adjacent column(s) installations to allow the grout to harden such that adequate tunnel support is provided by the jet-grout umbrella. The laboratory properties developed from this study may help designers and contractors attempting to optimize the installation sequence of a jet-grout umbrella. However, it should be remembered that in spite of the quality of these laboratory experiments, the in situ behaviour can present noticeable differences.

Acknowledgments

This work was supported by the Natural Sciences and Engineering Research Council of Canada.

References

Brill, G.T., Burke, G.K., Ringen, A.R., 2003. A ten year perspective of jet-grouting: advancements in applications and technology. In: Johnsen, L., Bruce, D.A., Byle, M. (Eds.), Proceedings of the 3rd International Conference – Grouting and Ground Treatment, New Orleans, vol. 1 of Geotechnical Special Publication No. 120, American Society of Civil Engineers, pp. 218–235.

Bruce, D.A., Boley, D.L., Gallavresi, F., 1987. New developments in ground reinforcement and treatment for tunnelling. In: Proceedings of 1987 Rapid Excavation and Tunnelling Conference, New Orleans. Society of Mining Engineers, Littleton, CO, pp. 811–835.

Bye, G.C., 1983. Portland cement: composition, production and properties. Pergamon Press, New York, 149p.

Coulter, S.N.P., 2004. Influence of tunnel jet-grouting on ground deformations at the Aescher Tunnel, Switzerland. Master's thesis, Department of Civil and Environmental Engineering, University of Alberta, Edmonton, Alta., Canada.

Croce, P., Flora, A., 2000. Analysis of single fluid jet-grouting. Géotechnique 50 (6), 739–750.

Fang, Y.-S., Liao, J.J., Lin, T.-K., 1994. Mechanical properties of jet-grouted soilcrete. Quarterly Journal of Engineering Geology 27 (3), 257–265.

Kauschinger, L.J., Hankour, R., Perry, E.B., 1992. Methods to estimate the composition of jet-grouted bodies. In: ASME Special Publication No. 30, American Society Mechanical Engineers, New Orleans, LA, USA, pp. 194–205.

Mussger, K., Koinig, J., Reischl, S., 1987. Jet-grouting in combination with NATM. In: Proceedings of Rapid Excavation and Tunnelling Conference, New Orleans. Society of Mining Engineers, Inc., Littleton, CO, pp. 292–308.

Pelizza, S., Peila, D., 1993. Soil and rock reinforcements in tunnelling. Tunnelling and Underground Space Technology 8 (3), 357–372.

Taylor, H.F.W., 1990. The Chemistry of Cements. Academic Press Inc., New York, 459p.